Chronic Hepatitis, Hepatocyte Fragility, and Increased Soluble Phosphoglycokeratins in Transgenic Mice Expressing a Keratin 18 Conserved Arginine Mutant

Nam-On Ku,*§ Sara Michie,‡§ Robert G. Oshima,‖ and M. Bishr Omary*§

Department of *Medicine and ‡Pathology, VA Palo Alto Health Care System, Palo Alto, California 94304; §The Digestive Disease Center, Stanford University School of Medicine, Stanford, California 94305; and ‖La Jolla Cancer Research Foundation, La Jolla, California 92037

Abstract. The two major intermediate filament proteins in glandular epithelia are keratin polypeptides 8 and 18 (K8/18). To evaluate the function and potential disease association of K18, we examined the effects of mutating a highly conserved arginine (arg89) of K18. Expression of K18 arg89→his/cys and its normal K8 partner in cultured cells resulted in punctate staining as compared with the typical filaments obtained after expression of wild-type K8/18. Generation of transgenic mice expressing human K18 arg89→cys resulted in marked disruption of liver and pancreas keratin filament networks. The most prominent histologic abnormalities were liver inflammation and necrosis that appeared at a young age in association with hepatocyte fragility and serum transaminase elevation. These effects were caused by the mutation since transgenic mice expressing wild-type human K18 showed a normal phenotype. A relative increase in the phosphorylation and glycosylation of detergent solubilized K8/18 was also noted in vitro and in transgenic animals that express mutant K18. Our results indicate that the highly conserved arg plays an important role in glandular keratin organization and tissue fragility as already described for epidermal keratins. Phosphorylation and glycosylation alterations in the arg mutant keratins may account for some of the potential changes in the cellular function of these proteins. Mice expressing mutant K18 provide a novel animal model for human chronic hepatitis, and for studying the tissue specific function(s) of K8/18.

CYTOPLASMIC intermediate filaments (IF)[1] are tissue and differentiation-state specific cytoskeletal proteins that have been well characterized in higher eukaryotes (reviewed by Steinert and Roop, 1988; Klymkowsky et al., 1989; Skalli and Goldman, 1991; Fuchs and Weber, 1994). All IF proteins have three common structural domains: a central α-helical "rod" domain of 310–350 amino acids which is flanked by non-α-helical NH_2-terminal "head" and COOH-terminal "tail" domains. Although the function(s) of IF proteins remain poorly understood, a role in maintaining cell integrity has emerged based on a number of human blistering skin diseases that are caused by point mutations in epidermal keratin IF proteins (reviewed by Fuchs and Coulombe, 1992; Steinert and Bale, 1993; Fuchs et al., 1994; McLean and Lane, 1995). An important breakthrough in the identification of IF related human diseases came after expressing a truncated epidermal keratin in transgenic mouse keratinocytes, with subsequent development of a disease resembling human epidermolysis bullosa simplex (EBS) (Vassar et al., 1991; Coulombe et al., 1991). Similarly, transgenic mice that over-express neurofilament-(NF)-L or NF-H (Xu et al., 1993; Cote et al., 1993) developed a neuromuscular disease that is similar to amyotrophic lateral sclerosis (ALS). Based on these latter animal models, several patients with sporadic ALS were subsequently found to have mutations in NF-H (Figlewicz et al., 1994).

In simple-type epithelia such as in the liver, exocrine pancreas, and intestine, the two major IF proteins are keratin (K) polypeptides 8 and 18 (K8/18) with variable expression of K19 and K20 (Moll et al., 1982, 1990, 1993; Calnek and Quaroni, 1993). K8 and K18 form obligate noncovalent heteropolymers which coalesce into a cytoplasmic filamentous meshwork that can also include other IF proteins that may be expressed in the same cells (Moll et al., 1982). K8 and K18 are phosphoglycoproteins with serine phosphorylation (Celis et al., 1983; Chou and Omary, 1993) and O-linked N-acetylglucosamine (GlcNAc) glycosylation (Chou et al., 1992). Phosphorylation of K8/18 in-

Address reprint requests to Nam-On Ku and other correspondence to M. Bishr Omary, VA Palo Alto Health Care System, 3801 Miranda Ave., 111 G.I., Palo Alto, CA 94304.

1. *Abbreviations used in this paper*: ALS, amyotrophic lateral sclerosis; EBS, epidermolysis bullosa simplex; EHK, epidermolytic hyperkeratosis; EN, epidermal nevi; EPPK, epidermolytic palmoplantar keratoderma; GlcNAc, N-acetylglucosamine; IF, intermediate filaments; K, keratin; NF, neurofilament; SGOT, serum glutamic-oxaloacetic transaminase; SGPT, serum glutamic-pyruvic transaminase; WT, wild type.

creases during the S and G2/M phases of the cell cycle (Chou and Omary, 1994) and plays an important role in keratin filament reorganization (Ku and Omary, 1994*a*). The function of K8/18 glycosylation is unknown although three human K18 head domain serine glycosylation sites were recently identified (Ku and Omary, 1995). No human disease is known to be associated with K8/18, and overexpression of wild type (WT) human K18 (Abe and Oshima, 1990) or K19 (Bader and Franke, 1990) in transgenic mice yields a normal phenotype. However, homozygous disruption of mouse K8 genes resulted in fetal death accompanied by extensive liver hemorrhage (Baribault et al., 1993), or in colonic hyperplasia, colitis, and rectal prolapse (Baribault et al., 1994) depending on the genetic background of the transgenic mice. In addition, ectopic expression of an epitope-tagged epidermal keratin as a transgene in mouse liver resulted in keratin filament disruption and hepatic inflammation (Albers et al., 1995).

More than 80 keratin mutations have been identified in human skin diseases, with >80% of the mutations involving two highly conserved regions located at the beginning and end of the rod domain (Coulombe and Fuchs, 1994; McLean and Lane, 1995). Of these two regions, the region that is proximal to the head domain contains a highly conserved arginine (arg) which is a "hot" mutation spot that accounts for nearly 40% of the identified mutations. Hence, this conserved arg is mutated in K14, K10, and K9 in the skin diseases EBS, epidermolytic hyperkeratosis (EH) and epidermolytic palmoplantar keratoderma (EPPK), respectively, in association with filament disruption. In addition, the mosaic disorder epidermal nevi (EN) of the epidermolytic hyperkeratosis type is also associated with mutation of the highly conserved arg of K10 (Paller et al., 1994). Our hypothesis was that tissue-specific transgenic mouse expression of human mutant K18, that has been altered at the conserved arg (arg89 of K18) could result in filament disruption and a potential disease phenotype in organs expressing this mutant protein. To test this hypothesis we first examined the effect of K18 arg89→cys/his mutations on filament assembly and showed that these mutations result in filament disassembly after expression in insect and mammalian cells. We then generated transgenic mice that express human K18 arg89→cys, and compared their phenotype to mice that express normal human K18. The mice that express mutant K18 developed chronic hepatitis and fragile livers in association with K8/18 filament disruption. In addition to causing filament disruption, the K18 arg mutation also resulted in an increase in the phosphorylation and glycosylation levels of the soluble fraction of K8/18 in transfected cells and in the transgenic animals. The significance of these findings is discussed.

Materials and Methods

Cell Culture and Reagents

Sf9 (insect ovarian) (PharMingen, San Diego, CA), NIH-3T3 (mouse fibroblast), HT29 (human colon), and NMuLi (mouse liver) (American Type Culture Collection, Rockville, MD) cells were cultured as recommended by the suppliers. Reagents used were: uridine diphosphate (UDP) - [4-5-^{3}H]-galactose, [6-^{3}H]-glucosamine-HCl, and orthophosphate ($^{32}PO_4$) (Dupont-New England Nuclear, Wilmington, DE); bovine milk galactosyltransferase (Sigma Chemical Co., St. Louis, MO); Baculo-Gold transfection kit (PharMingen); Transformer™ mutagenesis kit (Clontech, Palo Alto, CA); LipofectAMINE liposomes (GIBCO BRL, Gaithersburg, MD); enhanced chemiluminescence (ECL) kit (Amersham, Arlington Heights, IL). mAbs to human K8/18 were: L2A1 (Chou et al., 1992), CK5, and 8.13 (Sigma Chemical Co.). These antibodies recognize different epitopes of human K18 (mAb L2A1 and CK5) or human K8 and K18 (mAb 8.13). Rat mAb to mouse K8 (Troma I) was obtained from the National Institute of Child Health and Human Development. Polyclonal rabbit antibodies to human K8/18 (termed 8592) were generated after immunizing with K8/18 that was purified from the human colonic cell line HT29 using high salt extraction, and then ion exchange chromatography with a Mono-Q column.

Transfection and Construction of Mutants and Recombinant Viruses

Arg89 (codon CGC) of human K18 cDNA in a pBluescript SK$^+$ plasmid was mutated to cysteine (TGC) or histidine (CAC) using the Transformer kit as recommended by the manufacturer. Mutants were subcloned into the pVL1392 vector for expression in Sf9 cells or into the pMRB101 vector for expression in NIH-3T3 and NMuLi cells as described (Ku and Omary, 1994*a*). Generation of the baculovirus recombinants and transfection of mammalian cells were done as before (Ku and Omary, 1994*a*). Sf9 cells were cotransfected with linearized Baculo-Gold virus DNA, pVL1392-K8 and pVL1392-K18 (wild-type or arg→cys or arg→his K18 mutants). NIH-3T3 and NMuLi cells were co-transfected with pMRB101-K8 and pMRB101-K18 wild-type or mutant constructs using LipofectAMINE™ liposomes, as recommended by the manufacturer.

Isolation of Keratins

Keratins were isolated by immunoprecipitation from detergent solubilized cells or tissues, or using high salt extraction (Achtstaetter et al., 1986; Chou et al., 1993). For high salt extraction, cells or tissue fragments were homogenized with 1% Triton X-100 (TX-100), 5 mM EDTA in PBS, pH 7.4, for 2 min and centrifuged (16,000 *g*; 10 min; 4°C). The pellet was homogenized using a Dounce in high salt buffer containing 10 mM Tris-HCl (pH 7.6), 140 mM NaCl, 1.5 M KCl, 5 mM EDTA, 0.5% TX-100 (100 strokes). After a 30-min incubation at 4°C, the suspension was centrifuged and the insoluble keratin pellet was solubilized with SDS gel sample buffer. For immunoprecipitation, cells or tissue fragments were solubilized with 1% Empigen BB in PBS containing 5 mM EDTA, 0.1 mM phenylmethylsulfonyl fluoride, 25 μg/ml aprotinin, 10 μM leupeptin, 10 μM pepstatin, 0.5 μg/ml okadaic acid, 5 mM sodium pyrophosphate, and 50 mM NaF (45 min, 4°C) (Lowthert et al., 1995). After centrifugation, the supernatant was used for immunoprecipitation followed by SDS-PAGE (Laemmli, 1970).

Western Blotting and Indirect Immunofluorescence

Western blotting (Towbin et al., 1979) was done using samples separated by SDS-PAGE and then transferred to Immobilon-P membranes (Millipore Corp., Bedford, MA). The membranes were incubated with mAb L2A1 or CK5, or with rabbit anti-keratin antibody 8592 (1 h), washed, and then incubated with peroxidase-conjugated goat anti-mouse or anti-rabbit IgG. Keratin bands were visualized using enhanced chemiluminescence. Immunofluorescence was carried out as described (Ku and Omary, 1994*a*). Recombinant baculovirus infected Sf9 cells or transfected mammalian cells were grown on cover slips. After 2–3 d of baculovirus infection or 3 d of transient transfection, cells were fixed in methanol (−20°C, 3 min), incubated with mAb L2A1 (30 min, 22°C), washed, and then incubated with Texas red–conjugated goat anti-mouse antibody (30 min, 22°C). Fresh frozen mouse tissues were fixed then stained in a similar manner using mAb L2A1 or Troma I.

Radiolabeling and Tryptic Peptide Mapping

Cells or small mouse liver fragments were labeled with $^{32}PO_4$ for 5 h (250 μCi/ml) in phosphate-free media supplemented with 10% dialyzed fetal calf serum. Keratins were then isolated from the cells using high salt extraction or immunoprecipitation. The high salt extracted material represents the total keratin pool, whereas the immunoprecipitated material represents the detergent solubilized fraction. Glycosylation of K8/18 was assessed by galactosylation of accessible terminal GlcNAcs of K8/18 immunoprecipitates, using 0.6 μCi of UDP[^{3}H]galactose and 25 mU of galactosyltransferase in 20 μl reaction buffer (Chou et al., 1992). Tryptic glyco-

and phosphopeptide mapping was done as described (Boyle et al., 1991; Chou and Omary, 1993). For this, radiolabeled K18 (wild-type or mutant) was eluted from preparative SDS-PAGE gels, digested with trypsin, and then analyzed in the horizontal dimension by electrophoresis and in the vertical dimension by chromatography. Metabolic labeling of Sf9 cells with [^{3}H]glucosamine was done exactly as described (Ku and Omary, 1994*b*).

Construction of the Genomic K18 Arg Mutant and Generation of Transgenic Mice

Mutant K18 cDNA (arg89→cys) was digested with AlwN I to produce a 250-bp fragment that contains the K18 mutation. A Kpn I-Xho I 4-kb fragment of the genomic K18 pGC1853 plasmid (Abe and Oshima, 1990) was ligated with a 2.9-kb Kpn I-Xho I fragment of pBluescript SK+ that lacks an AlwN I site. The generated 6.9-kb K18-containing DNA was digested with AlwN I to remove K18 DNA that contains the region coding for arg89 and generate a 6.7-kb species. The 6.7-kb fragment was ligated with the 250-bp fragment containing the K18 mutation. The generated DNA (~7 kb) was digested with Kpn I and Xho I to produce a 4-kb fragment (containing the K18 arginine mutation) which was then ligated with the remaining 9-kb Kpn I-Xho I fragment of pGC1853. The 13-kb product was digested with Hind III and the 10-kb K18 genomic fragment containing the arg mutation was then used for injection into pronuclei of fertilized FVB/N mouse eggs. Transgene copy number was estimated using tail DNA that was isolated from progeny of the founder mice using dot blot hybridization of multiple dilutions of the tail DNA with human K18 cDNA as described (Abe and Oshima, 1990). Densitometric scanning was done to quantitate the copy number using a standard curve of K18 plasmid DNA.

Transgenic Lines, Liver Perfusion, and Blood Testing

All transgenic lines were housed in the same room with strict infection-control precautions. Serum was tested monthly from randomly chosen mice and no evidence of infection was detected which included testing for murine viral hepatitis. Four transgenic mouse lines were used for breeding and the described experiments. One line expressed wild type human K18 (termed TG2) and was described previously (Abe and Oshima, 1990). The three other lines are termed F22, F30, and F50 which express the arg89→cys human K18 transgene (collectively called K18C). For liver perfusion and blood testing, F22, F30, and F50 heterozygous mice (2–4-mo old) were used and all three lines gave similar results. Age-matched TG2 and nontransgenic mice were used as a source of control livers. Prior to organ harvesting, mice were killed by CO_2 inhalation. Liver perfusion was carried out using 0.025% collagenase type I (Worthington Biomedical Corporation, Freehold, NJ) as described (Clayton and Darnell, 1983). Cell viability was determined using trypan blue exclusion. For blood testing, ~0.4 ml of blood was collected from age matched transgenic mice that do not carry the K18 transgene (five mice), TG2 (six mice) which made up the control group (11 mice); and from heterozygous K18C mice (six F22, three F30, and three F50). From this, 0.1 ml was used to obtain a complete blood count, and the remaining was used for serum testing of creatinine, total protein, albumin, alkaline phosphatase, lipase, serum glutamic-oxaloacetic (SGOT) and glutamic-pyruvic transaminase (SGPT).

Results

Effect of Human K18 Arg89→his/cys Mutations on K8/18 Filament Assembly in Insect and Mammalian Cells

We tested two K18 arg89 mutations, arg→cys (RΔC) and arg→his (RΔH), which have been reported in several patients with EBS (K14 mutations), EHK and EN (K10 mutations), and EPPK (K9 mutations) (reviewed by Fuchs et al., 1994; McLean and Lane, 1995). Wild type, RΔH, or RΔC K18 were coexpressed with their wild type heteropolymeric counterpart K8 in insect Sf9 cells after infection with recombinant baculovirus constructs. We chose to initially test these constructs in Sf9 cells since this system allows us to obtain large quantities of K8/18 for biochemical analysis including sufficient material for tryptic peptide mapping. In addition, we previously showed that the glycosylation and phosphorylation of human K18 expressed in Sf9 cells, in terms of labeled peptides, is nearly identical to what is observed in mammalian cells (Ku and Omary, 1994*a,b*). As shown in Fig. 1 *A* (lanes *1–3*), significant amounts of K8/18 were expressed, as determined using high salt extraction followed by Coomassie staining. High salt extraction provides >90% recovery of all the expressed K8 and K18 (Chou et al., 1993). Expression of K8/18 was also confirmed by immunoprecipitation using de-

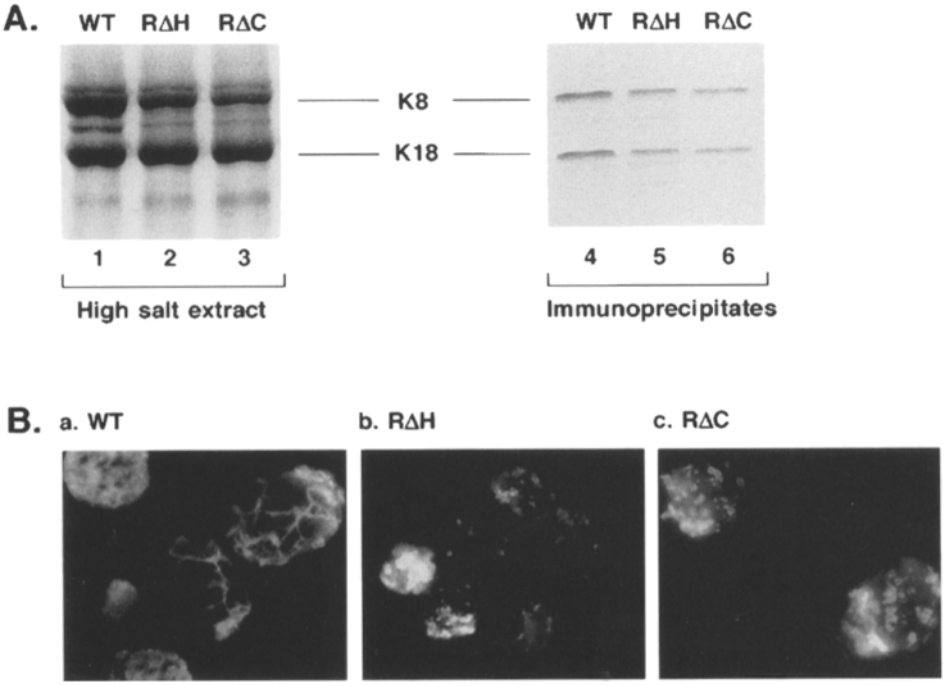

Figure 1. The K18 arg89→cys/his mutants form disrupted filaments when co-expressed with wild-type K8 in Sf9 cells. (*A*) Equivalent numbers of Sf9 cells were infected with recombinant wild type K8/K18 or WT K8/K18RΔH or WT K8/K18RΔC baculoviruses for four days. Cells were then processed for high salt extraction (lanes *1–3*), or for immunoprecipitation with mAb L2A1 (lanes *4–6*) as described in Materials and Methods. The panel shows a Coomassie stain after SDS-PAGE. (*B*) Sf9 cells were grown on cover slips then infected for two days with the recombinant baculovirus constructs used in *A*. Cells were then fixed and stained by indirect immunofluorescence using mAb L2A1 as described in Materials and Methods.

tergent solubilized cells that are identical to those used for lanes *1–3* (Fig. 1 *A*, lanes *4–6*). We then analyzed the nature of K8/18 filaments formed in Sf9 cells using immunofluorescence staining. Expression of WT K8/18 in Sf9 cells results in formation of disorganized rope-like filaments (Ku and Omary, 1994*b*; and Fig. 1 *B*, *a*). In contrast, expression of WT K8 with the RΔH or RΔC K18 mutants resulted in formation of dot/inclusion-like patterns (Fig. 1 *B*, *b* and *c*) that were distinctly different than the pattern observed after expression of WT K8/18 (Fig. 1 *B*, *a*).

We tested if K18 arg mutations in mammalian cells also result in filament disruption when co-transfected with WT K8, similar to what was observed in Sf9 cells. As shown in Fig. 2, *a* and *d*, transfection of WT K8/18 into mouse NIH-3T3 fibroblast or liver NMuLi cells, which contain vimentin and keratins as their endogenous IF, respectively, showed the expected filamentous staining pattern. In contrast, transfection of WT K8 and RΔH or RΔC K18 into both cell lines resulted in a punctate nonfilamentous pattern (Fig. 2), similar to what was observed in Sf9 cells (Fig. 1 *B*), and consistent with inability of the filaments to assemble properly.

Development and Analysis of Transgenic Mice that Express Human arg→cys K18

To study the effect of the highly conserved arginine in the context of a whole animal, we used a 10-kb human K18 genomic clone (Kulesh and Oshima, 1989) to introduce a single base substitution in exon 1 that converted arg89 to cys (K18C). This genomic construct resulted in formation of disrupted filaments when co-transfected with WT K8 into NIH-3T3 cells (not shown, but a pattern similar to that in Fig. 2 *b*). The K18C genomic DNA was injected into mouse embryos and three founder lines (termed F22, F30, and F50) were bred to produce the progeny used for further analysis. Incorporation of the human K18 10-kb transgene was confirmed by Southern blotting (not shown). The K18 transgene copy number/cell for the three heterozygous K18C lines relative to transgenic mice that express the WT K18 gene (termed TG2; Abe and Oshima, 1990) was 10, 12, and 18, respectively. The TG2 mice (heterozygous copy number = 17) were used as control in our studies and were the same strain (FVB/N) as the F22, F30, and F50 mice.

Our in vitro transfection experiments (Fig. 2) suggested that K18 arg89 mutations may behave in a dominant negative manner and result in filament disruption. We used immunofluorescence staining to examine filament organization in several tissues isolated from TG2 mice that express WT human K18 or from F22, F30 and F50 mice that express mutant K18C. As shown in Fig. 3, TG2 hepatocytes have normal appearing filaments after staining using mAb L2A1 (*a*) which recognizes human K18, or after staining with mAb Troma I which recognizes endogenous mouse K8 (*e*). The L2A1 antibody does not crossreact with mouse keratins (not shown but see Fig. 4). In contrast, staining of hepatocytes from transgenic mice F22 and F30 (Fig. 3, *b*, *f*, and *g*) and F50 (not shown) using either antibody showed a dramatic alteration in filament staining. There was maintenance of staining at the cell perimeter but complete or near complete disruption of cytoplasmic staining. A similar loss of the cytoplasmic filamentous staining pattern was also noted in the pancreas with replacement by a fine dot pattern and retention of the apical

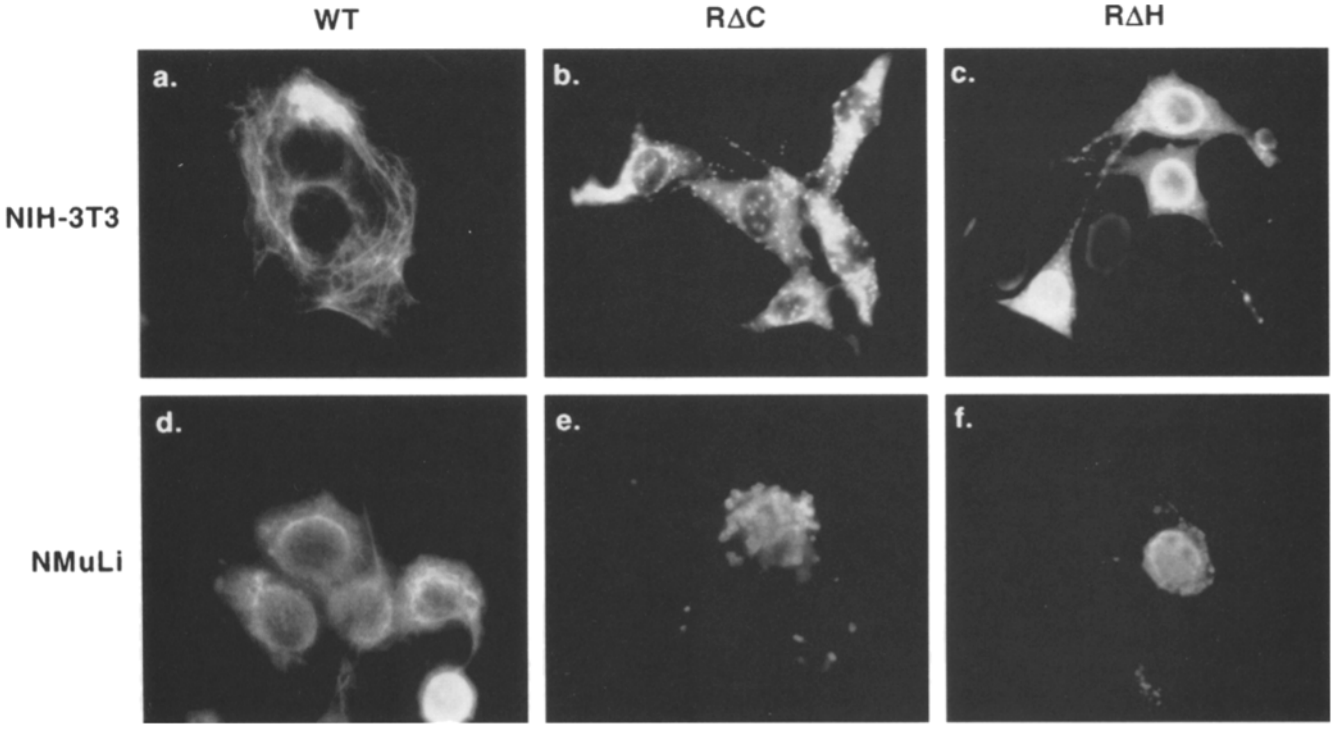

Figure 2. Immunofluorescence of transfected wild-type K8/18, and wild-type K8/mutant K18 expressed in mammalian cells. NIH-3T3 and NMuLi cells were transiently co-transfected with WT K8/18 or with WT K8/K18RΔH or RΔC. After 3 d, cells were fixed and analyzed by indirect immunofluorescence using mAb L2A1 as described in Materials and Methods.

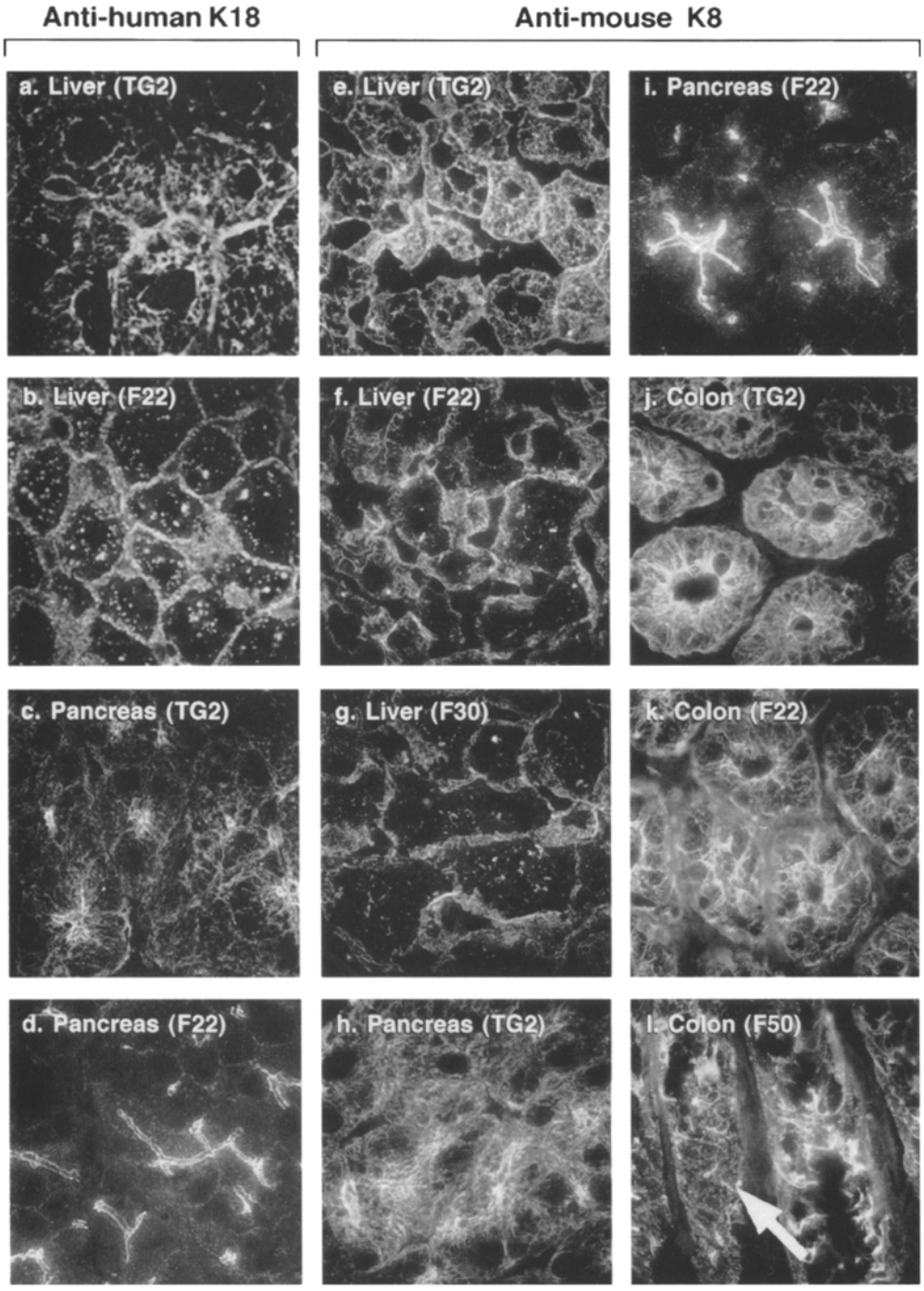

Figure 3. Immunofluorescence of keratin assembly in transgenic mouse liver, pancreas and colon expressing wild type and mutant human K18. Tissues taken from mice expressing WT human K18 (TG2) or arg89→cys K18 (F22, F30, F50) were immediately frozen in O. C. T. compound. Frozen sections were cut, fixed briefly in cold acetone, then stained using mouse anti–human K18 (mAb L2A1) or rat anti–mouse K8 (mAb Troma I) antibodies in phosphate buffered saline containing 2.5% bovine serum albumin. After rinsing, sections were incubated with Texas red conjugated goat anti–mouse or anti–rat antibodies, respectively. Tissues were visualized using a fluorescence microscope with a 100× objective lens. Slides taken with Ektachrome 400 film were scanned using a Leafscan 45™ scanner (Leaf System Inc., Southboro, MA). White arrow (panel *l*) shows punctate keratin staining pattern in colon. No staining was noted in non-transgenic mouse liver, pancreas, and colon using mAb L2A1 (not shown).

ductal staining (Fig. 3, compare *c* and *h* with *d* and *i*). However, minimal disruption of K8/18 filaments was noted in the colon of F22 mice (Fig. 3 *k*) with disruption becoming more prominent with increasing copy number in the F50 mice (Fig. 3 *l*). The filament disruption noted in the pancreas and liver of the K18C mice was age independent and involved the majority of cells, with only few cells manifesting a normal appearing filament staining pattern (not shown).

We used high salt extraction (HSE) or immunoprecipitation with mAb L2A1 to compare the level of expression of human K18C transgene to that of the endogenous K18 gene in K18C mice, and to that of the human WT K18 transgene in TG2 mice. Given that human K18 also forms heteropolymers with endogenous mouse K8/18, immunoprecipitation using mAb L2A1 allows for the preferential isolation of detergent solubilized human K18 together with complexed endogenous mouse keratins, whereas high salt extraction provides a near quantitative recovery of the total keratin pool. As shown in Fig. 4 *A*, mAb L2A1 specifically immunoprecipitated keratins from detergent solubilized liver, pancreas and colon from mice expressing WT human K18 (lane *2*) or K18C (lanes *3–5*) but not from normal nontransgenic mice (lane *1*). The human K18 transgene product co-migrates with human K18 isolated from HT29 cells, and human K8 migrates slightly faster than

mouse K8 (Fig. 4 *A*, compare lanes *2–6* with lane *7*). Colonocytes in culture (from human HT29 cells, Fig. 4 *A*, lane *7*) or isolated from fresh mouse tissues (Fig. 4 *A*, lane *5*) also express K19 which co-immunoprecipitates with K8/18.

In order to assess the relative levels of expression of human K18 versus endogenous mouse K18, analysis of the total keratin pool using high salt extraction was carried out. As shown in Fig. 4 *B*, the relative ratio of human to mouse K18 is nearly 3:1 in TG2 mice (lane *2*) whereas the ratio in F22 mice is only 1:2 (lane *3*). In the case of HSE of liver from F50 and F30 mice, the relative levels of human versus mouse K18 are nearly equal, and the absolute total keratin per gram tissue was reproducably lower than that obtained from TG2 or F22 mice (Fig. 4 *B*), presumably due to the amount of liver inflammation/necrosis (see below) and/or differences in protein turnover. This indicates that the K18C transgene is behaving in a dominant negative fashion, and that the filament disruption noted in K18C mice is related to the arg mutation and not simply to K18 overexpression. Verification of the assignment of the individual bands obtained after HSE was carried out by Western blotting using antibodies specific for mouse K8 (Troma I), human K18 (CK5), and a rabbit polyclonal antibody (8592) that recognizes mouse and human K18 (Fig. 4 *B*). Of note, in contrast to the K18 protein levels in the liver (F22 > F30 > F50, Fig. 4 *B*), the protein level of K18 in colon of the F50 mice was more than that in the F22 and F30 mice but similar to the level in the TG2 mice (not shown). Hence, it appears that the hK18 protein levels correlate with the transgene copy number, with more keratin degradation occurring in liver than colon, due to the lack of "protection" based on the absence in hepatocytes of other type I keratins (e.g., K19 in colonocytes). The decreased level of mK18 in the K18C and TG2 livers is very likely due to the degradation of both mK18 and hK18, which are in excess of the limiting amounts of mK8 as shown previously by transfection experiments (Kulesh et al., 1989).

Histologic and intact-tissue examination of liver, kidney, lung, gall bladder, pancreas, colon and small intestine from F22, F30, and F50 mice revealed changes only in the liver (Fig. 5). Inspection of intact livers showed increased prominence of the vascular subcapsular markings, with appearance of a punctate pattern rather than a meshwork vascular pattern, in older (≥6 mo) F50 (Fig. 5 *b*), F22 and F30 mice (not shown) compared with age matched TG2 (Fig. 5 *a*) or nontransgenic mice (not shown). Microscopic liver examination showed a chronic inflammatory infiltrate (Fig. 5 *d*) which was nonregionalized and patchy (not shown) with areas of necrosis (Fig. 5 *e*). These findings were noted in liver sections of mice as early as one month of age, and were absent in TG2 mice (Fig. 5 *c*). Trichrome staining showed lack of fibrosis in mice up to nine months old although necrosis and bleeding into necrotic (Fig. 5 *f*) and nonnecrotic areas became highly prominent as the mice aged (Fig. 5, *g* and *h*). Furthermore, collagenase liver perfusion of young K18C and TG2 mice, at an early stage when inflammation and necrosis are mild or minimal, resulted in significant cell death only in K18C mice (mean cell viability was % 21 ± 3 [$n = 6$] and % 90 ± 5 [$n = 4$] for K18C and TG2 mice, respectively), which supports the noted progressive necrosis and is consistent with an increase in the fragility of the K18C livers. The histologic findings of inflammation and necrosis were also supported by serologic testing which showed a statistically significant twofold transaminase elevation in the K18C as compared

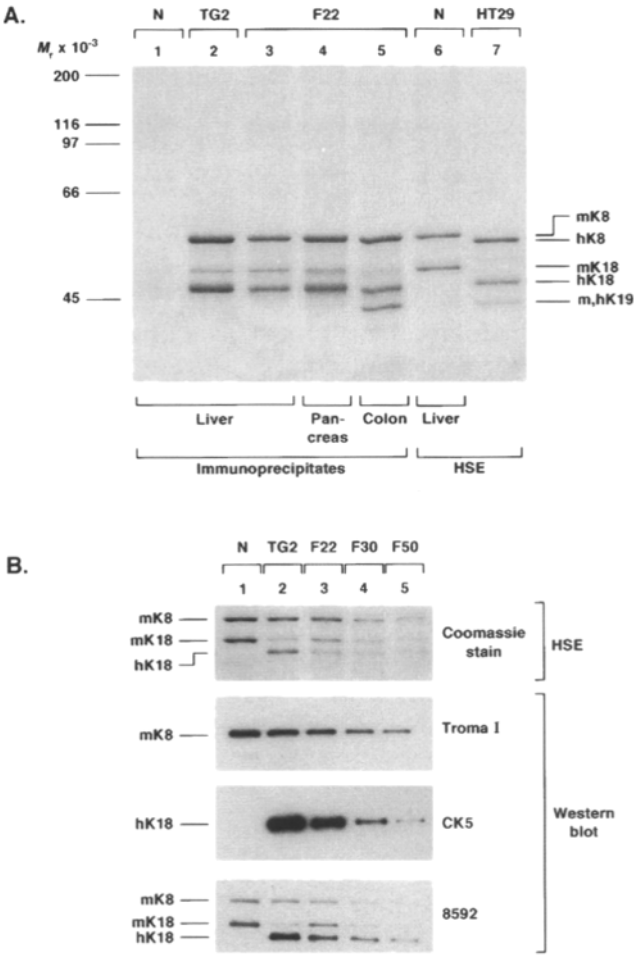

Figure 4. Analysis of wild type and mutant human K18 expression in transgenic mice. (*A*) Indicated organs were obtained from TG2 and K18C transgenic mice, or from non-transgenic FVB/N mice (*N*). Tissues were homogenized in phosphate buffered saline containing 1% Empigen, 5 mM EDTA, 10 μM leupeptin, 10 μM pepstatin, 25 μg/ml aprotinin and 0.1 mM phenylmethylsulfonyl fluoride. After solubilization (45 min, 4°C), nonsolubilized material was removed by pelleting followed by immunoprecipitation using mAb L2A1 as described in Materials and Methods. The immunoprecipitated proteins were compared to normal mouse K8/18 (mK8 and mK18 isolated from normal mice) or human K8/18 (hK8 and hK18 isolated from the colonic human cell line HT29) which were purified using high salt extraction (*HSE*). Mouse (*F22* colon) and human (*HT29* cells) K19 is also indicated. (*B*) 1 g of liver tissue was removed from the indicated mice followed by HSE and SDS-PAGE analysis of equivalent fractions, then Coomassie blue staining. Triplicate gels were transferred to polyvinylidene difluoride membranes followed by immunoblotting using mAb Troma I (specific for mouse K8), CK5 (specific for human K18) or rabbit polyclonal antibody 8592 which was raised against purified human K8 and 18 but as shown cross reacts with mouse K8 and K18. Immunoblotting of total liver cell lysates (5 μg of protein per liver, after homogenizing then solubilizing in 2% SDS sample buffer) from the above mouse lines with Troma I and 8592 antibodies gave identical results (not shown).

with TG2 or nontransgenic mice (Table I). The extent of transaminase elevation is mild but similar to elevations noted in patients with chronic liver disease (Ellis et al., 1978). No significant difference was noted in white cell, platelet or red blood cell counts (not shown) or in other serum chemistry tests (Table I).

Effect of human K18 arg89 Mutations on K8/18 Phosphorylation and Glycosylation

The altered filament organization of K8/K18RΔC or RΔH expressed in Sf9 cells raised the possibility that concurrent alteration in K8/18 phosphorylation and/or glycosylation may also occur. This is based on the observed filament reorganization in association with K8/18 hyperglycosylation and/or hyperphosphorylation in several systems including cell cycle progression through the S and G2/M phases (Chou and Omary, 1994) and heat stress (Liao et al., 1995*b*). We tested this by comparing the specific activity of these modifications in WT K8/18 versus WT K8 and RΔH K18 isolated by immunoprecipitation from detergent solubilized cells. Phosphorylation was assessed by in vivo labeling with $^{32}PO_4$, and glycosylation was assessed by galactosylation of accessible terminal GlcNAcs using galactosyltransferase and UDP[^{3}H]galactose, and by metabolic labeling using [^{3}H]glucosamine. As shown in Fig. 6 *A*, when equal amounts of K8/18 immunoprecipitates isolated from $^{32}PO_4$-labeled Sf9 cells expressing WT or RΔH K18 were analyzed, a marked increase in the specific activity of K8/ mutant K18 phosphorylation was noted. An increase in the glycosylation specific activity of K8/mutant K18 isolated from cells expressing K18 arg89→his (Fig. 6 *A*, compare lanes *c* and *d*) was also noted. A similar increase in the glycosylation and phosphorylation of K8/K18RΔC was obtained as compared with WT K8/18 immunoprecipitates (not shown). Furthermore, these increases were noted using polyclonal and a panel of monoclonal K8/18 antibodies (not shown), indicating that the observation is independent of an antibody–antigen phenomenon. In addition, metabolic labeling of Sf9 cells with [^{3}H]glucosamine provided similar results (not shown) to those obtained by in vitro galactosylation (Fig. 6 *A*).

Analysis of the tryptic glyco- and phosphopeptide maps of immunoprecipitated WT versus RΔH K18 (Fig. 6 *B*) or RΔC K18 (not shown) demonstrated that the modified peptides were identical. Similarly, analysis of the tryptic glyco- and phosphopeptides of K8 isolated from Sf9 cells infected with recombinant baculovirus containing WT K8/ 18 or WT K8/K18RΔH were also identical (not shown). In contrast to the detergent solubilized material which constitutes only a small fraction of the expressed total keratin pool in Sf9 cells, when phosphorylation of the entire high salt extract keratin pool was analyzed, only a small increase (1.4×) was noted between WT and RΔC or RΔH K18 (not shown). This indicates that the increase in specific activity of K8/18 phosphorylation and glycosylation occurs preferentially in the soluble fraction after mutation of K18 arg89. Analysis of K8/18 phosphorylation and glycosylation in NIH-3T3 cells transfected with WT K8/18 or WT K8/RΔH K18 showed a similar increase in the specific activity of both modifications (Fig. 7, compare lanes *4* with *3* and lanes *6* with *5*) as observed in Sf9 cells (Fig. 6). A significant but less dramatic increase in the phosphorylation and glycosylation of detergent solubilized K8/18, isolated from TG2 or K18C mice, was also noted (Fig. 7 *B*). The increase in K8/18 phosphorylation involved only the relatively small pool of detergent soluble keratin since two-dimensional isoelectric focusing/SDS-PAGE analysis of K8/18 HSE samples obtained from TG2 and F22 mouse livers did not show any significant shifts in K8 or K18 isoelectric forms (not shown).

Discussion

Importance of the Highly Conserved arg in IF Protein Assembly

The first finding of this study is that the highly conserved arginine 89 of human K18, which is found in most type I keratins and in many other IF proteins including NF-H, vimentin, lamins, nestin, desmin and peripherin, plays an important role in filament assembly in vivo. Support for this includes the filament reorganization observed in association with mutation of the conserved arg89 of K18 in recombinant baculovirus infected insect cells (Fig. 1), transfected mammalian cells (Fig. 2), and liver and pancreas of trangenic mice (Fig. 3). This adds a glandular keratin (i.e., K18) to the epidermal keratins (K14, K10, and K9) for which this arg plays a critical in vivo role in filament assembly. The importance of this arg in filament assembly is evident in patients with the skin diseases involving mutation of this residue (EBS, EHK, EN, EPPK) (reviewed by Fuchs et al., 1994; McLean and Lane, 1995) and is supported by cell culture transfection experiments of K14 arg125→cys (Coulombe et al., 1991) or lamin A arg41→his (Heald and McKeon, 1990). In addition, earlier evidence for the general importance of arg residues in IF assembly was obtained by metabolic labeling of vimentin-expressing cultured cells with the arg analog canavanine (Moon and Lazarides, 1983) or by in vitro deimination of arg residues (Inagaki et al., 1989) which resulted in the inability of the modified vimentin to incorporate into filaments.

The findings of this study indicate that expression of arg89→cys K18 in transgenic mice, at levels that are less than those in mice expressing WT K18, manifests a dominant negative phenotype, particularly in the liver and pancreas which express K8/18 as their primary IF proteins. The less pronounced filament disruption noted in the colon (and small intestine, not shown) is potentially related to a "dilution" effect by K19 and K20 which are expressed at varying levels in the intestine (Moll et al., 1993; Calnek and Quaroni, 1993). Although significant K8/18 filament reorganization was noted in the pancreas, we did not observe any histologic changes. In addition, the normal lipase (Table I) and glucose levels (mean glucose of 211 ± 28 for the control group and 200 ± 44 mg/dL for the K18C group, $n = 8$ per group) in the K18C mice support the lack of pancreatic inflammation and diabetes, respectively. This differs from the ectopic expression of epidermal keratins in transgenic mouse pancreatic islet cells which resulted in significant diabetes and early mortality (Blessing et al., 1993). At this stage, we do not know why the pancreas was histologically spared in the K18C mice except for the possibility of functional redundancy by other proteins that

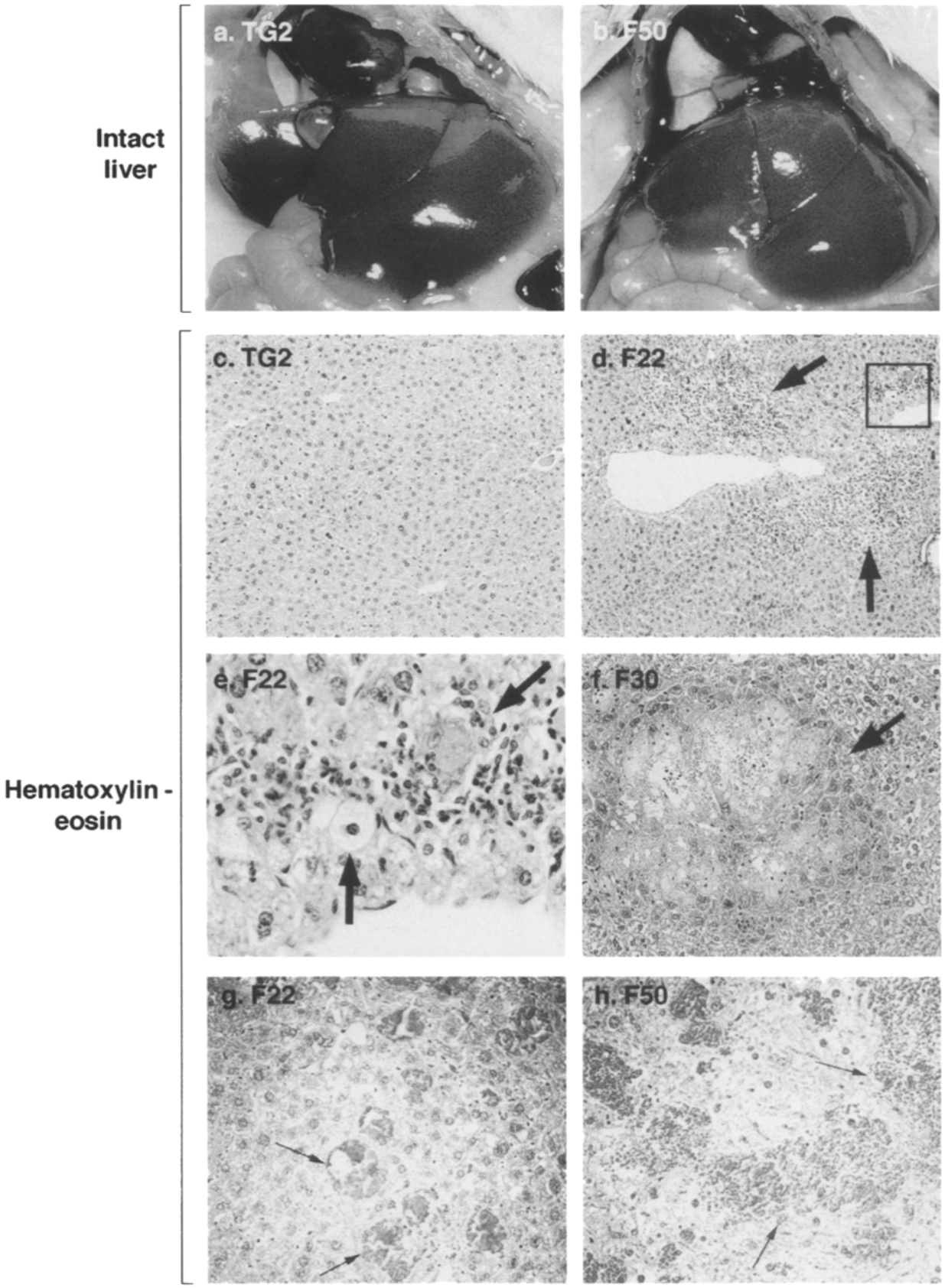

Figure 5. Pathology of transgenic mouse livers. Mice were euthanized by CO_2 inhalation. Livers from 9-mo-old mice (*a* and *b*) were photographed without any manipulation. Alternatively, livers from 2-mo-old (*c–e*) or 9-mo-old (*f–h*) mice were formalin-fixed, paraffin-embedded, sectioned, and stained using hematoxylin-eosin (*c–h*). *e* is an enlargement of the area in *d* enclosed by a square. Arrows indicate: mononuclear chronic inflammatory infiltrate (*d*), degenerating hepatocytes (*e*), extensive necrosis (*f*) and scattered areas of hemorrhage (*g* and *h*).

Table I. Serum Chemistry Analysis of Control and K18 arg→cys Transgenic Mice

Test	Control (n = 11)	Transgenic (n = 12)	Transgenic / Control	Significant difference
Cr	0.28	0.28	1.00	No
Alk Phos	138.00	145.00	1.05	No
Total protein	4.50	5.00	1.11	No
Albumin	2.47	2.42	0.98	No
Lipase	1,043.00	1,051.00	1.01	No
SGOT	125.00	238.00	1.90	Yes (0.04)
SGPT	87.00	180.00	2.07	Yes (0.01)

Approximately 400 ul of blood was collected from control and K18C mice as described in Materials and Methods. The serum was separated then used for the following analysis: Cr (creatinine mg/dL); Alk phos (alkaline phosphatase U/L); total protein and albumin (g/dL); lipase (U/L); SGOT (serum glutamic-oxaloacetic transaminase U/L) and SGPT (serum glutamic-pyruvic transaminase U/L). Panel shows mean values of indicated tests. Significant difference indicates $p < 0.05$.

would offset K8/18 disruption in the pancreas. Histologic sparing of the pancreas was also noted in the K8 null mice (Baribault et al., 1993, 1994) which lends support to a functional redundancy hypothesis for certain K8/18 functions in some organs. Regardless, the K18C and TG2 transgenic mice will provide useful animal models for studying potential K8/18 tissue specific functions in a number of organs despite the presence or absence of any histologic changes.

Alteration of K8/18 Phosphorylation and Glycosylation Secondary to the K18 arg89 Mutation

Mutation of the highly conserved arg results in abolishment of a potential consensus phosphorylation site (RXX*S* to C/HXX*S*, S = ser-92 in K18) for a number of kinases including calmodulin-dependent protein kinase and protein kinase C (Pearson and Kemp, 1991). However, in the case of K18, there is no detectable phosphorylation or glycosylation of this serine (data not shown) which is conserved in type I and II keratins but not in other IF proteins. It is not known if this serine is phosphorylated in the epidermal keratins, although the nine characterized phosphorylation sites of K1 (Steinert, 1988) do not include this serine. In addition, in vivo IF phosphorylation regions identified to date exclude the rod domain and, instead, involve the head, tail, or head/tail domains (e.g., Evans, 1988; Ku and Omary, 1994*a*).

Although a clear consequence of the arg mutation is filament disruption and secondary cell fragility, it is unclear if other cellular functions of keratins also become affected. The difficulty is that clear-cut functions for IF proteins remain elusive and, therefore, full understanding of the physiologic significance of the arg mutation is not yet within reach given our current limited functional and mechanistic information. To that end, the relative enrichment of phosphoglyco-K8/18 in the detergent solubilized fraction could indicate that a small but potentially functionally significant fraction of K8/18 becomes available, or ceases to become available for interaction with putative IF associated proteins (depending on the nature of the interaction of a given IF associated protein). For example, in vitro phosphorylation of plectin or lamin B by protein kinase A or C result in a significant decrease in the plectin–lamin B interaction (Foisner et al., 1991). With regard to the single O-GlcNAc type of K8/18 glycosylation, its function is unclear although it is a dynamic modification (Kearse and Hart, 1991; Chou et al., 1992) that is found in cytoplasmic and nuclear proteins involved in protein-protein interaction (reviewed by Haltiwanger et al., 1992). It remains to be determined if modulation of the phosphoglyco-K8/18 soluble pool or if the arg89 mutation per se play a role in K8/18 interaction with associated proteins. For example, a recently described ATP dependent interaction of K8/18 with the 70-kD heat shock proteins occurs preferentially with the soluble fraction of K8/18 (Liao et al., 1995*a*).

Transgenic Mice that Express K18 arg89→cys Serve as a Model for Human Chronic Hepatitis and for Studying K18 Function(s)

Chronic inflammation in the livers of K18C transgenic mice provides an animal model for chronic hepatitis and raises the possibility that some cases of human chronic hepatitis may in fact be caused by mutations in K18. To that end, 10–33% of patients with chronic liver disease and cirrhosis have an "idiopathic" or cryptogenic form of liver disease (Conn and Atterbury, 1993; Greeve et al., 1993). Our hypothesis is supported by several transgenic animal models that express deleted forms of K14 and K10 in keratinocytes, with resultant skin disease phenotypes (e.g., Vassar et al., 1991; Fuchs et al., 1994). In addition, the number of keratins that are involved in human disease is accumulating so that at this stage it may be more appropriate to ask what disease(s) do mutations in K18 cause, rather than could mutations in K18 cause any human disease. The keratins that are involved in human disease to date include: K5, K14, K1, K10, K9, K2e (reviewed by Fuchs et al., 1994; McLean and Lane, 1995), K16, K17 (McLean et al., 1995), and K6a (Bowden et al., 1995). The keratin-associated diseases together with mutations in NF-H that have been associated with ALS (Figlewicz et al., 1994) can result in autosomal dominant and recessive, mosaic, and sporadic diseases. Therefore, testing patients with "idiopathic" chronic liver disease for the presence of K18 mutations should clarify the potential role of K18 in this disease. Other candidate chronic liver diseases to consider that may involve mutations in K18 include familial cirrhosis (Maddrey and Iber, 1968) and Indian childhood cirrhosis (Adamson et al., 1992) which are familial, and autoimmune type hepatitis (reviewed by Mieli-Vergani and Vergani, 1994) which is sporadic.

Abnormal aggregation of K8/18-containing complexes in hepatocytes, in the form of Mallory bodies (Mallory, 1911; and reviews by Jensen and Gluud, 1994*a*, *b*), is noted in several liver diseases, particularly alcoholic liver disease. We did not observe any Mallory body formation in the K18C transgenic mice (not shown), but it is possible that mutations in K18 could predispose to toxin induced liver injury. Although it is not clear if the initial event in K18C mouse livers is necrosis (likely due to cell fragility) or inflammation or both, the observations of liver fragility upon collagenase perfusion and bleeding into necrotic areas as the mice age are prominent features. Therefore, as has been clearly demonstrated for the epidermal keratins, a role in the maintenance of tissue integrity is also likely to extend to simple epithelial keratins. Such a role does not exclude other potential tissue specific functions that remain to be explored.

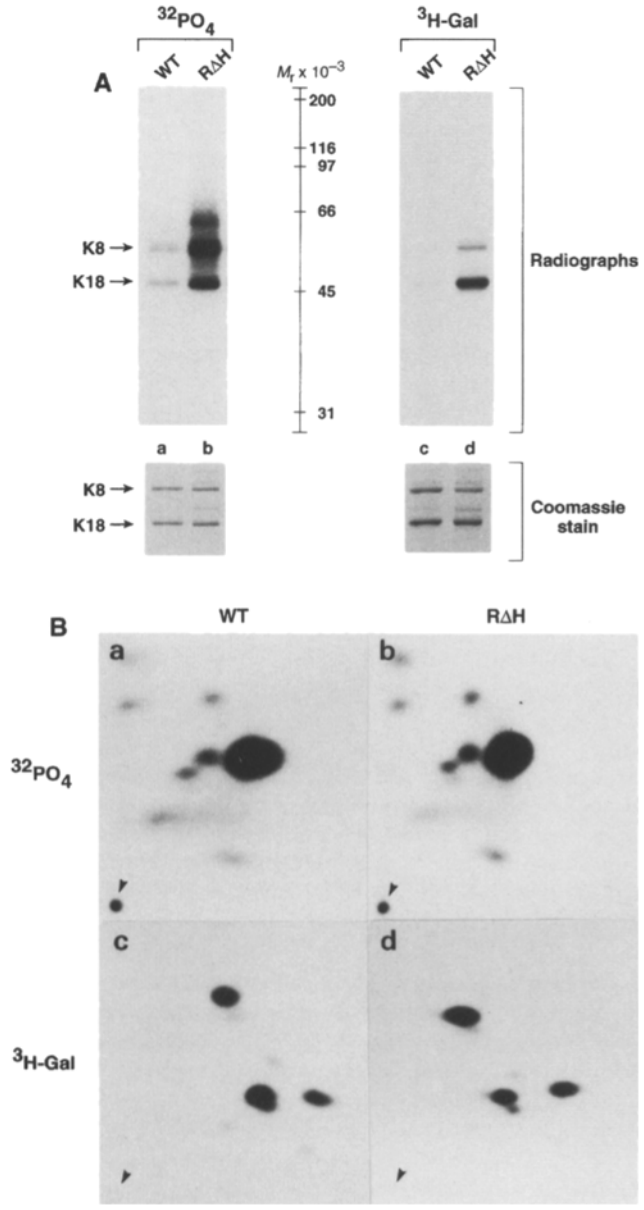

Figure 6. The detergent solubilized fraction of arg→his K18 is hyperphosphorylated and hyperglycosylated, and displays similar tryptic glyco- and phosphopeptides as compared with WT K18. (*A*) Sf9 cells were infected with a baculovirus recombinant containing WT K8/18 or WT K8/K18RΔH in duplicate dishes. One dish was labeled with $^{32}PO_4$ for 5 h during the fourth day of infection followed by immunoprecipitation of K8/18 as described in Materials and Methods. Immunoprecipitates were also obtained from the non-labeled duplicate dishes followed by galactosylation using galatosyltransferase and UDP[^{3}H]galactose. The amount of immunoprecipitated K8/18 were normalized so that equal amounts were loaded on the gel. (*B*) [^{32}P]phosphate or [^{3}H]galactose labeled K18 were purified using preparative SDS-PAGE followed by electroelution of the individual K18 bands. After trypsinization, samples were analyzed by electrophoresis in the horizontal direction and chromatography in the vertical direction. 10,000 cpm were spotted (position indicated by *arrowhead*) for each of the maps. Exposure was 14 d for the ^{3}H maps and 1 d for the ^{32}P maps.

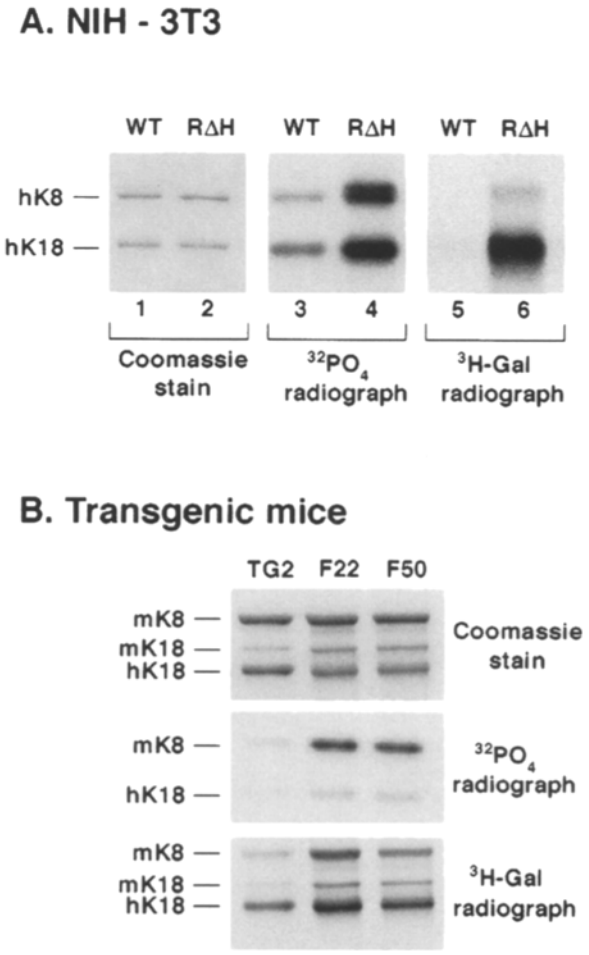

Figure 7. Phosphorylation and glycosylation of WT K8/18 and WT K8/arg mutant K18 expressed in NIH-3T3 cells or isolated from transgenic mice livers. (*A*) Transiently transfected NIH-3T3 cells expressing the indicated constructs were set up in duplicate 100 mm dishes. One set was labeled with $^{32}PO_4$ for 5 h followed by immunoprecipitation of K8/18. The second nonlabeled set was used for K8/18 immunoprecipitation then galactosylation using UDP[^{3}H]galactose. The immunoprecipitated K8/18 that was analyzed by SDS-PAGE was normalized so that equal amounts of the WT and RΔH containing immunoprecipitates were loaded. Lanes *1* and *2* show the Coomassie stained gel of the radiograph in lanes *3* and *4*. The Coomassie stained gel for the ^{3}H-labeled samples was similar to that in lanes *1* and *2* (not shown). (*B*) Livers were isolated from heterozygous TG2, F22, and F50 transgenic mice (~2-mo-old). One lobe of each liver was cut into small pieces using a razor blade then labeled with $^{32}PO_4$ for 5 h followed by immunoprecipitation. A second lobe of each liver was homogenized in detergent then processed by immunoprecipitation followed by galactosylation using UDP[^{3}H]galactose as described in Materials and Methods. *m*, mouse; *h*, human.

Comparison of the Phenotypes of K18C Mice with K8 Null and Ectopic K14 Expressing Transgenic Mice

The observed phenotype in our K18C mice is similar but more severe than that observed in transgenic mice that express a substance P epitope-tagged K14, which was targeted to the liver using a transthyretin gene promoter and enhancer elements (Albers et al., 1995). The similarities

include the presence of liver inflammation, keratin filament disruption, and lack of Mallory bodies. It is not known if the transgenic mice that express K14 manifest increased liver fragility and hemorrhage. However, any differences between the two phenotypes may be accounted for by differences in the type (K18 versus K14) and/or level of expressed keratin transgene, or in the mouse strain used to express the transgene.

Liver abnormalities were also noted in the K8 null mice, but varied depending on the mouse strain. For example, C57/Bl K8 null mice that died at a late embryonic stage had extensive liver hemorrhage (Baribault et al., 1993) that was more significant but reminiscent to the spontaneous parenchymal microscopic bleeding noted in the K18C mice. In contrast, the FVB/N K8 null mice (i.e., same strain as the K18C mice) developed mild hepatitis and necrosis, but the major phenotype included female sterility, embryonic lethality of some animals and colorectal pathology (Baribault et al., 1994), with the latter three findings not seen in the K18C heterozygous mice (not shown). Interestingly, filament disruption in the K18C mice appeared to occur preferentially in the central regions of the cell while sparing filaments near the plasma membrane (Fig. 3), which may reflect increased stability of filaments associated with membrane associated proteins such as desmosomal components. Such an effect is seen in doubly targeted mK8 embryonic stem cells, where mK18 is lost due to degradation except for the cell periphery with apparent association with desmosomes (Baribault and Oshima, 1991). This effect is also seen in the intestine of the mK8 null FVB/N mice (Baribault et al., 1994). Of note, phosphorylated K18 appears to be preferentially associated with the basolateral surfaces of normal human hepatocytes and with the apical regions of pancreatic cells, perhaps implying a favored association or stabilization of phosphorylated keratin filaments with membrane structures (Liao et al., 1995*c*). Electron microscopy of K18C liver specimen also showed association of keratin filaments with desmosomal structures (not shown) although relative quantitation of intracellular versus peripheral filaments was not done.

All the effects that we observed in the K18 arg89 mutant transgenic mice can be specifically attributed to the arg mutation since expression of the wild type human K18, at levels higher than the mutant K18, generated a normal phenotype. The full spectrum of the K18C transgenic mice phenotype will be further evaluated as homozygous mice are generated and crossbreeding into additional strains is carried out.

We are very grateful to Linda P. Jacob for preparing the manuscript, Kris Morrow and Sally Morefield for preparing the figures, Dr. Rosemary Broom for veterinary advice, Daniel Brown for assistance with tissue sectioning and immunofluorescence, Janet R. Maynard and Ron Van Groningen for serum testing.

This work was supported by Veterans Administration Merit Awards (S. Michie, M. B. Omary), NIH grant DK47918 (M. B. Omary), NCI grant CA94302 (R. G. Oshima) and Digestive Disease Center Grant DK38707. N.-O. Ku is a recipient of an American Heart Association California Affiliate postdoctoral fellowship.

Received for publication 3 August 1995 and in revised form 7 September 1995.

References

Abe, M., and R. G. Oshima. 1990. A single human keratin 18 gene is expressed in diverse epithelial cells of transgenic mice. *J. Cell Biol.* 111:1197–1206.

Achtstaetter, T., M. Hatzfeld, R. A. Quinlan, D. C. Parmelee, and W. W. Franke. 1986. Separation of cytokeratin polypeptides by gel electrophoretic and chromatographic techniques and their identification by immunoblotting. *Methods Enzymol.* 134:355–371.

Adamson, M., B. Reiner, J. L. Olson, Z. Goodman, L. Plotnick, I. Bernardini, and W. A. Gahl. 1992. Indian childhood cirrhosis in an American child. *Gastroenterology.* 102:1771–1777.

Albers, K. M., F. E. Davis, T. N. Perrone, E. Y. Lee, Y. Liu, and M. Vore. 1995. Expression of an epidermal keratin protein in liver of transgenic mice causes structural and functional abnormalities. *J. Cell Biol.* 128:157–169.

Bader, B. L., and W. W. Franke. 1990. Cell type-specific and efficient synthesis of human cytokeratin 19 in transgenic mice. *Differentiation.* 45:109–118.

Baribault, H., and R. G. Oshima. 1991. Polarized and functional epithelia can form after the targeted inactivation of both mouse keratin 8 alleles. *J. Cell Biol.* 115:1675–1684.

Baribault, H., R. Price, K. Miyai, and R. G. Oshima. 1993. Mid-gestational lethality in mice lacking keratin 8. *Genes & Dev.* 7:1191–1202.

Baribault, H., J. Penner, R. V. Iozzo, and M. Wilson-Heiner. 1994. Colorectal hyperplasia and inflammation in keratin 8-deficient FVB/N mice. *Genes & Dev.* 8:2964–2973.

Blessing, M., U. Ruther, and W. W. Franke. 1993. Ectopic synthesis of epidermal cytokeratins in pancreatic islet cells of transgenic mice interferes with cytoskeletal order and insulin production. *J. Cell Biol.* 120:743–755.

Bowden, P. E., J. L. Haley, A. Kansky, J. A. Rothnagel, D. O. Jones, and R. J. Turner. 1995. Mutation of a type II keratin gene (K6a) in pachyonychia congenita. *Nature Genet.* 10:363–365.

Boyle, W. J., P. Van Der Geer, and T. Hunter. 1991. Phosphopeptide mapping and phosphoamino acid analysis by two-dimensional separation on thin layer cellulose plates. *Methods Enzymol.* 201:110–149.

Calnek, D., and A. Quaroni. 1993. Differential localization by in situ hybridization of distinct keratin mRNA species during intestinal epithelial cell development and differentiation. *Differentiation.* 53:95–104.

Celis, J. E., P. M. Larsen, S. J. Fey, and A. Celis. 1983. Phosphorylation of keratin and vimentin polypeptides in normal and transformed mitotic human epithelial amnion cells: behavior of keratin and vimentin filaments during mitosis. *J. Cell Biol.* 97:1429–1434.

Chou, C-F., and M. B. Omary. 1993. Mitotic-arrest associated enhancement of O-linked glycosylation and phosphorylation of human keratins 8 and 18. *J. Biol. Chem.* 268:4465–4472.

Chou, C-F., and M. B. Omary. 1994. Mitotic arrest with anti-microtubule agents or okadaic acid is associated with increased glycoprotein terminal GlcNAc's. *J. Cell Sci.* 107:1833–1843.

Chou, C.-F., C. L. Riopel, L. S. Rott, and M. B. Omary. 1993. A significant soluble keratin fraction in "simple" epithelial cells: lack of an apparent phosphorylation and glycosylation role in keratin solubility. *J. Cell Sci.* 105:433–445.

Chou, C.-F., A. J. Smith, and M. B. Omary. 1992. Characterization and dynamics of O-linked glycosylation of human cytokeratin 8 and 18. *J. Biol. Chem.* 267:3901–3906.

Clayton, D. F., and J. E. Darnell. 1983. Changes in liver-specific compared to common gene transcription during primary culture of mouse hepatocytes. *Mol. Cell Biol.* 3:1552–1561.

Conn, H. O., and C. E. Atterbury. 1993. Diseases of the liver. L. Schiff and E. R. Schiff, editors. J.B. Lippincott Co., 898 pp.

Cote, F., J.-F. Collard, and J.-P. Julien. 1993. Progressive neuronopathy in transgenic mice expressing the human neurofilament heavy gene: a mouse model of amyotrophic lateral sclerosis. *Cell.* 73:35–46.

Coulombe, P. A., and E. Fuchs. 1994. Molecular mechanisms of keratin gene disorders and other bullous diseases of the skin. *In* Molecular Mechanisms of Epithelial Cell Junctions: from Development to Disease. S. Citi, editor. R. G. Landes Co. 259–285.

Coulombe, P. A., M. E. Hutton, A. Letai, A. Hebert, A. S. Paller, and E. Fuchs. 1991. Point mutations in human keratin 14 genes of epidermolysis bullosa simplex patients: Genetic and functional analyses. *Cell.* 66:1301–1311.

Ellis, G., D. M. Goldberg, R. J. Spooner, and A. M. Ward. 1978. Serum enzyme tests in diseases of the liver and biliary tree. *Am. J. Clin. Pathol.* 70:248–258.

Evans, R. M. 1988. The intermediate-filament proteins vimentin and desmin are phosphoylated in specific domains. *Eur. J. Cell Biol.* 46:152–160.

Figlewicz, D. A., A. Krizus, M. G. Martinoli, V. Meininger. M. Dib, G. A. Rouleau, and J.-P. Julien. 1994. Variants of the heavy neurofilament subunit are associated with the development of amyotrophic lateral sclerosis. *Hum. Mol. Genet.* 3:1757–1761.

Foisner, R., P. Traub, and G. Wiche. 1991. Protein kinase A- and protein kinase C-regulated interaction of plectin with lamin B and vimentin. *Proc. Natl. Acad. Sci. USA.* 88:3812–3816.

Fuchs, E., Y.-m. Chan, A. S. Paller, and Q.-C. Yu. 1994. Cracks in the foundation: keratin filaments and genetic disease. *Trends Cell Biol.* 4:321–326.

Fuchs, E., and P. A. Coulombe. 1992. Of mice and men: genetic skin diseases of keratin. *Cell.* 69:899–902.

Fuchs, E., and K. Weber. 1994. Intermediate filaments: structure, dynamics, function and disease. *Annu. Rev. Biochem.* 63:345–382.

Greeve, M., L. Ferrell, M. Kim, C. Combs, J. Roberts, N. Ascher, and T. L.

Wright. 1993. Cirrhosis of undefined pathogenesis: absence of evidence for unknown viruses or autoimmune processes. *Hepatology.* 17:593–598.

Haltiwanger, R. S., W. G. Kelly, E. P. Roquemore, M. A. Blomberg, L.-Y. D. Dong, L. Kreppel, T.-Y. Chou, and G. W. Hart. 1992. Glycosylation of nuclear and cytoplasmic proteins is ubiquitous and dynamic. *Biochem. Soc. Trans.* 20:264–269.

Heald, R., and R. McKeon. 1990. Mutations of phosphorylation sites in lamin A that prevent nuclear lamina disassembly in mitosis. *Cell.* 61:579–589.

Inagaki, M., H. Takahara, Y. Nishi, K. Sugawara, and C. Sato. 1989. Ca^{2+}-dependent deimination-induced disassembly of intermediate filaments involves specific modification of the amino-terminal head domian. *J. Biol. Chem.* 264:18119–18127.

Jensen, K., and C. Gluud. 1994*a*. The Mallory body: Morphological, clinical and experimental studies (part 1 of a literature survey). *Hepatology.* 20:1061–1077.

Jensen, K., and C. Gluud. 1994*b*. The Mallory body: Theories on development and pathological significance (part 2 of a literature survey). *Hepatology.* 20: 1330–1342.

Kearse, K. P., and G. W. Hart. 1991. Lymphocyte activation induces rapid changes in nuclear and cytoplasmic glycoproteins. *Proc. Natl. Acad. Sci. USA.* 88:1701–1705.

Klymkowsky, M. W., J. B. Bachant, and A. Domingo. 1989. Functions of intermediate filaments. *Cell Motil. & Cytoskel.* 14:309–331.

Ku, N.-O., and M. B. Omary. 1994*a*. Identification of the major physiologic phosphorylation site of human keratin 18: potential kinases and a role in filament reorganization. *J. Cell Biol.* 127:161–171.

Ku, N.-O., and M. B. Omary. 1994*b*. Expression, glycosylation, and phosphorylation of human keratins 8 and 18 in insect cells. *Exp. Cell Res.* 211:24–35.

Ku, N.-O., and M. B. Omary. 1995. Identification and mutational analysis of the glycosylation sites of human keratin 18. *J. Biol. Chem.* 270:11820–11827.

Kulesh, D. A., and R. G. Oshima. 1989. Complete structure of the gene for human keratin 18. *Genomics.* 4:339–347.

Kulesh, D. A., G. Cecena, Y. M. Darmon, M. Vasseur, and R. G. Oshima. 1989. Posttranslational regulation of keratins: degradation of mouse and human keratins 18 and 8. *Mol. Cell Biol.* 9:1553–1565.

Laemmli, U. K. 1970. Cleavage of structural proteins during the assembly of the head of bacteriophage T4. *Nature (Lond.).* 227:680–685.

Liao, J., L. A. Lowthert, N. Ghori, and M. B. Omary. 1995*a*. The 70-kDa heat shock proteins associate with glandular intermediate filaments in an ATP-dependent manner. *J. Biol. Chem.* 270:915–922.

Liao, J., L. A. Lowthert, and M. B. Omary. 1995*b*. Heat stress or rotavirus infection of human epithelial cells generates a distinct hyperphosphorylated form of keratin 8. *Exp. Cell Res.* 219:348–357.

Liao, J., L. A. Lowthert, N.-O. Ku, R. Fernandez, and M. B. Omary. 1995*c*. Dynamics of human keratin 18 phosphorylation: polarized distribution of phosphorylated keratins in simple epithelial tissues. *J. Cell Biol.* 131:1291–1301.

Lowthert, L. A., N.-O. Ku, J. Liao, P. A. Coulombe, and M. B. Omary. 1995. Empigen BB: a useful detergent for solubilization and biochemical analysis of keratins. *Biochem. Biophys. Res. Commun.* 206:370–379.

Maddrey, W. C., and F. L. Iber. 1964. Familial cirrhosis: a clinical and pathological study. *Ann. Int. Med.* 61:667–679.

Mallory, F. B. 1911. Cirrhosis of the liver. Five different types of lesions from which it may arise. *Bull. Johns Hopkins Hosp.* 22:69–75.

McLean, W. H. I., and E. B. Lane. 1995. Intermediate filaments in disease. *Curr. Opin. Cell Biol.* 7:118–125.

McLean, W. H. I., E. L. Rugg, D. P. Lunny, S. M. Morley, E. B. Lane, O. Swensson, P. J. C. Dopping-Hepenstal, W. A. D. Griffiths, R. A. J. Eady, C. Higgins, H. A. Navsaria, I. M. Leigh, T. Strachan, L. Kunkeler, and C. S. Munro. 1995. Keratin 16 and keratin 17 mutations cause pachyonychia congenita. *Nature Genet.* 9:273–278.

Mieli-Vergani, G., and D. Vergani. 1994. Progress in pediatric autoimmune hepatitis. *Semin. Liver Dis.* 14:282–288.

Moll, R., W. W. Franke, D. L. Schiller, B. Geiger, and R. Krepler. 1982. The catalog of human cytokeratins: patterns of expression in normal epithelia, tumors and cultured cells. *Cell.* 31:11–24.

Moll, R., D. L. Schiller, and W. W. Franke. 1990. Identification of protein IT of the intestinal cytoskeleton as a novel type I cytokeratin with unusual properties and expression patterns. *J. Cell Biol.* 111:567–580.

Moll, R., R. Zimbelmann, M. D. Goldschmidt, M. Keith, J. Laufer, M. Kasper, P. J. Koch, and W. W. Franke. 1993. The human gene encoding cytokeratin 20 and its expression during fetal development and in gastrointestinal carcinomas. *Differentiation.* 53:75–93.

Moon, R. T., and E. Lazarides. 1983. Canavanine inhibits vimentin assembly but not its synthesis in chicken embryo erythroid cells. *J. Cell Biol.* 97:1309–1314.

Paller, A. S., A. J. Syder, Y.-M. Chan, Q.-C. Yu, E. Hutton, G. Tadini, and E. Fuchs. 1994. Genetic and clinical mosaicism in a type of epidermal nevus. *N. Engl. J. Med.* 331:1408–1415.

Pearson, R. B., and B. E. Kemp. 1991. Protein kinase phosphorylation site sequences and consensus specificity motifs: tabulations. *Methods Enzymol.* 200:61–81.

Skalli, O., and R. D. Goldman. 1991. Recent insights into the assembly, dynamics, and function of intermediate filament networks. *Cell Motil. & Cytoskeleton.* 19:67–79.

Steinert, P. M., and S. J. Bale. 1993. Genetic skin diseases caused by mutations in keratin intermediate filaments. *Trends Genet.* 9:280–284.

Steinert, P. M. 1988. The dynamic phosphorylation of the human intermediate filament keratin 1 chain. *J. Biol. Chem.* 263:1333–1339.

Steinert, P. M., and D. R. Roop. 1988. Molecular and cellular biology of intermediate filaments. *Ann. Rev. Biochem.* 57:593–625.

Towbin, H., T. Staehelin, and J. Gordon. 1979. Electrophoretic transfer of proteins from polyacrylamide gels to nitrocellulose sheets: procedures and some applications. *Proc. Natl. Acad. Sci. USA.* 76:4350–4354.

Vassar, R., P. A. Coulombe, L. Degenstein, K. Albers, and E. Fuchs. 1991. Mutant keratin expression in transgenic mice causes marked abnormalities resembling a human genetic skin disease. *Cell.* 64:365–380.

Xu, Z., L. C. Cork, J. W. Griffin, and D. W. Cleveland. 1993. Increased expression of neurofilament subunit NF-L produces morphological alterations that resemble the pathology of human motor neuron disease. *Cell.* 73:23–33.